

Temporally resolved Raman backscattering diagnostic of high intensity laser channeling

T. G. Jones

Plasma Physics Division, Naval Research Laboratory, Washington, DC 20375

K. Krushelnick

Department of Physics, Imperial College, University of London, London SW7 2BZ, United Kingdom

A. Ting

Plasma Physics Division, Naval Research Laboratory, Washington, DC 20375

D. Kaganovich

Hebrew University, Jerusalem, Israel

C. I. Moore

Plasma Physics Division, Naval Research Laboratory, Washington, DC 20375

A. Morozov

Department of Mechanical and Aerospace Engineering, Princeton University, Princeton, New Jersey 08543

(Received 10 July 2001; accepted for publication 11 March 2002)

The implementation of an innovative technique for measuring the propagation of intense laser pulses through plasma channels is described. At high laser intensities, temporally resolved stimulated Raman backscattering can be used to diagnose both the electron density and the laser intensity inside the plasma channel, observations which are not possible using other techniques. This diagnostic is demonstrated in experiments using an open-ended capillary in which a plasma channel was created. The plasma channel was generated using either an electrical discharge or laser ablation by a second laser pulse. © 2002 American Institute of Physics. [DOI: 10.1063/1.1475348]

I. INTRODUCTION

Recent advances in laser technology have enabled experiments using laser pulses focused to extremely high intensity ($I \geq 10^{19}$ W/cm²) thus making possible the exploration of parameter regimes in both atomic and plasma physics.¹ Aside from phenomena which can be examined with these laser systems, there are potentially important applications of very high intensity light—in particular, advanced particle acceleration techniques,² coherent x-ray generation,³ and inertial confinement fusion.⁴

However, while present lasers are capable of producing focused intensities of the required magnitude for these applications, the volume over which such high fields exist is not large, since it is usually necessary to focus the beam to a very small spot—which consequently results in short diffraction distances. Thus, proposed applications for high intensity lasers will only become practical if the length over which the beam maintains its focused intensity can be extended significantly. In fact, channeling of high intensity light should also be a useful technique for more fundamental physics experiments, since nonlinear effects such as harmonic generation, self-phase modulation, and plasma instabilities associated with the propagation of high intensity laser light may be studied more easily. Another consideration for applications of this technology is that such channeling be uniform—especially for harmonic generation and x-ray lasers where the coherence of the output x rays is important.

In an underdense plasma, channeling of laser pulses is possible if an appropriate radial variation in the index of

refraction η can be produced across the laser profile. The index of refraction (for radiation of frequency, ω) in a plasma is given by

$$\eta^2 = 1 - \frac{\omega_{pe}^2}{\omega^2},$$

where $\omega_{pe} = (4\pi n_e e^2/m_e)^{1/2}$ is the electron plasma frequency, n_e is the plasma electron density, and m_e is the mass of the plasma electron. For a cylindrical volume of plasma, a radial variation in the refractive index of the plasma which is centrally peaked can produce focusing or “channeling,” similar to the effect produced by an optical fiber.

In a plasma, the laser pulse itself can induce a modification of the refractive index and, e.g., “self-guiding” effects can be produced due to the relativistic mass increase of electrons oscillating in a very high intensity laser field. The effective mass of plasma electrons decreases towards the edge of the laser pulse (the lower intensity regions) thus producing a maximum in the refractive index on axis. For a Gaussian intensity profile, self-focusing develops from this relativistic effect if the power of the laser pulse exceeds a critical value; i.e., $P_{crit} = 17(\omega_{pe}/\omega_0)^2$ GW.⁵ This phenomenon has been observed in some recent experiments,⁶ although relativistic self-guiding can be significantly complicated due to the many other processes which occur simultaneously at very high laser intensities such as (i) ponderomotive self-focusing (cavitation and filamentation),⁷ (ii) ionization induced refraction,^{8–10} (iii) atomic nonlinear self-focusing,¹¹ beam

breakup (self-modulation),¹² (v) laser hosing,¹³ and (vi) pulse-front erosion.¹⁴

However, if a preformed plasma channel, having an electron density minimum on axis, can be formed prior to the interaction, laser pulses of lower power may also be guided successfully with a significant reduction in these complicating effects. Recent work suggests that such plasma channels may be the ideal medium for laser accelerator,¹⁵ x-ray laser,^{16,17} and high harmonic generation applications.¹⁸

The preparation of such channels is an active area of research. They have been produced using several techniques such as (i) the hydrodynamic motion of a plasma created by a relatively low intensity laser pulse,^{19–21} (ii) the ponderomotive force and Coulomb expulsion in the focal region of a high intensity laser pulse,²² (iii) hollow glass waveguides,²³ and (iv) capillary discharges.^{24–26}

Many of the difficulties of high intensity laser plasma interaction experiments are due to the extremely short time scales and the nonlinearity of these interactions. It is particularly difficult to make precise measurements of the laser intensity and the plasma density profile during the interaction in order to compare with theoretical models. Measurements of the local plasma density in a guiding channel have been made previously using interferometry^{27,28} and Thomson scattering.²⁹ These techniques work well in a gas jet plasma channel, however, since Thomson scattering requires a clear side view of the plasma, and interferometry in addition requires a uniform or symmetric plasma, they are not suited to capillary plasma channels. In this article, we discuss experiments performed at the U.S. Naval Research Laboratory in which we use an innovative diagnostic technique to study the propagation of intense laser pulses in a plasma channel. In particular, by making temporally resolved Raman backscatter measurements we are able to measure the propagation of an intense laser pulse through a preformed channel created in an open-ended capillary. Our experiments utilize two methods of generating capillary plasmas: (1) a capillary discharge device and (2) plasma ablated from the capillary walls by a second, relatively low intensity laser pulse.

In this article, Sec. II briefly discusses these two techniques of generating capillary plasmas. Section III discusses measurements of stimulated Raman backscattering and Sec. IV provides details of how such measurements were implemented to diagnose propagation of intense laser pulses in a plasma channel. Finally Sec. V concludes with a discussion of these results.

II. PLASMA CHANNEL FORMATION

Extended propagation of terawatt (TW) laser pulses has been shown in plasma channels formed with a capillary discharge.²⁵ These discharges can be operated on relatively long time scales (microseconds) so that it may also be possible to channel relatively long duration, high energy laser pulses using this method. Capillary discharges are typically operated in high vacuum and therefore can be easily diagnosed via x-ray and visible spectroscopy.

However, capillary discharge-formed channels have been measured to have densities $\sim 10^{19}$ cm⁻³ or higher.³⁰

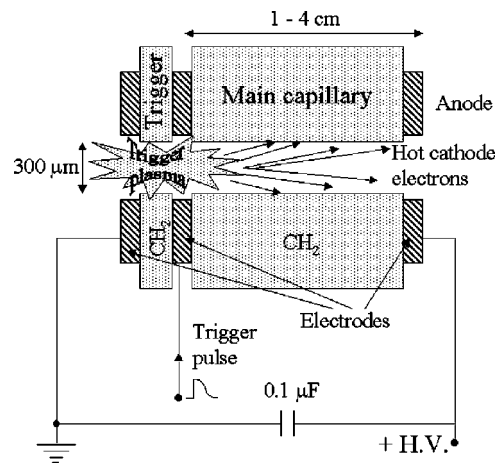


FIG. 1. Schematic diagram of capillary discharge device.

The standard laser wakefield acceleration (LWFA) scheme requires lower densities for which the plasma period, $\tau_p = 2\pi/\omega_{pe} \sim \tau_L$, where τ_L is the laser pulse length. For a laser pulse length of 400 fs, the matching density is $\sim 10^{17}$ cm⁻³. Furthermore, discharge-formed capillary plasma channels are maintained by plasma currents of several hundred amps, generating magnetic fields on the order of 1 T. Such magnetic fields would likely cause an increase in the electron beam emittance and would be detrimental for laser plasma acceleration. Laser ablated capillary plasmas are free of discharge-generated magnetic fields, and have been measured to have $n_e \sim 10^{18}$ cm⁻³. While guiding of TW laser pulses by laser-ablated capillary plasmas has yet to be demonstrated, these characteristics are promising for application to guiding for laser acceleration in general and for standard LWFA in particular. Generation of capillary plasmas by laser ablation has been used previously in x-ray laser experiments.¹⁶ Our capillary laser ablation experiments aim to develop this plasma generation technique for optical guiding of TW laser pulses and ultimately, laser acceleration of particles.

The basic components of a capillary discharge are shown in Fig. 1. Typically, the device consists of an insulating dielectric material in which a small diameter hole has been drilled. Electrodes are placed at the ends of the capillary tube. A low jitter discharge can be initiated by setting a dc voltage between the electrodes and triggering the main discharge with a laser or a smaller discharge at one end. The timing jitter of the discharge is an important parameter for experiments requiring the synchronization of a plasma discharge with an ultrashort, high intensity laser pulse. Synchronization was achieved by triggering the discharge, the Pockels cell of the laser which produced the injected pulse, and the diagnostic electronics from an adjustable electronic delay generator. The discharge initiation jitter was at least 20 ns and was inherent to the electronics used, however it was unimportant due to the long duration of the discharge.

The duration and current, and hence the plasma parameters, are determined by the capacitors connected across the capillary and the resistance of the discharge circuit, each of which can be varied. The voltage characteristics during the discharge were monitored using a high voltage probe at-

tached to one of the electrodes and the current was measured using a Rogowski coil situated around an electrical feed to a capillary electrode. The typical discharge current rise time in our experiments was ~ 200 ns. The charge voltage was set so that total discharge energy was less than 1 J.

Our capillary discharge devices were constructed using polyethylene, with capillary diameters ranging from 300–500 μ , and with lengths to 2 cm. For laser guiding experiments, polyethylene was used exclusively since it is composed solely of carbon and hydrogen. A high intensity laser pulse should therefore experience less defocusing from ionization-induced refraction during propagation through the resulting low Z plasma.

During discharge initiation, a surface flashover occurs along the inner capillary wall and a plasma is formed which is composed of electrons and ions ablated from the wall material. The initial plasma moves inwards from the surface before equilibrium is established. In long time scale discharges ($\tau_d \gg 1 \mu s$), the pressure profile across the diameter of the capillary becomes approximately constant due to high radial thermal conductivity at the typical currents ($\sim \text{few} \times 100$ A). The pressure can be equilibrated by shock waves on a time scale, $\tau \sim d/2c_s$ [where the sound speed, $c_s = (\gamma k T_i / m_e)^{1/2}$] which is much faster than the plasma flow.³¹ We estimate this time for our experimental conditions to be less than 10 ns. Since thermal transport produces a radially peaked temperature and conductivity profile, the plasma current is concentrated along the axis of the capillary. A radially peaked temperature profile produces a plasma density minimum on axis as plasma pressure is equilibrated [$N_e(r) \sim 1/T_e(r)$]. Therefore, $\eta(r)$ was peaked on axis, providing an optically guiding plasma channel.

The details of the capillary discharge device used in our experiments has been discussed in greater detail elsewhere.²⁴ The design was modular such that different capillaries could be interchanged and damaged capillaries could be quickly replaced. Symmetry of the discharge is clearly an important requirement for these experiments. For asymmetric discharges, the effect of the capillary plasma is to refract an injected laser pulse into the walls of the capillary or to generate higher order spatial modes in the beam profile during passage through the plasma. Laser pulses are also subject to absorption and scattering by the capillary plasma and these effects are of particular interest in our experiments.

The experimental setup for capillary plasma formation by laser ablation is shown in Fig. 2(a). Two lasers are used to produce pulses separated in time and frequency. A laser ablation pulse at a wavelength of 532 nm was followed by a guided “probe” pulse at a wavelength of 1054 nm. The 1054 nm pulse was then available as a guided probe pulse at high intensities, and as an imaging beam at lower intensities. Ablation pulses with duration \sim few ns and energy up to 300 mJ were used in these experiments. Characteristics of the transmitted probe pulse could then be measured after filtering out the ablation pulse with color filters.

A cylindrically symmetric plasma, expanding radially inward from the capillary walls, is desired as a guiding plasma channel. Experiments with subpicosecond laser ablation in a capillary have revealed that a hollow density profile can be

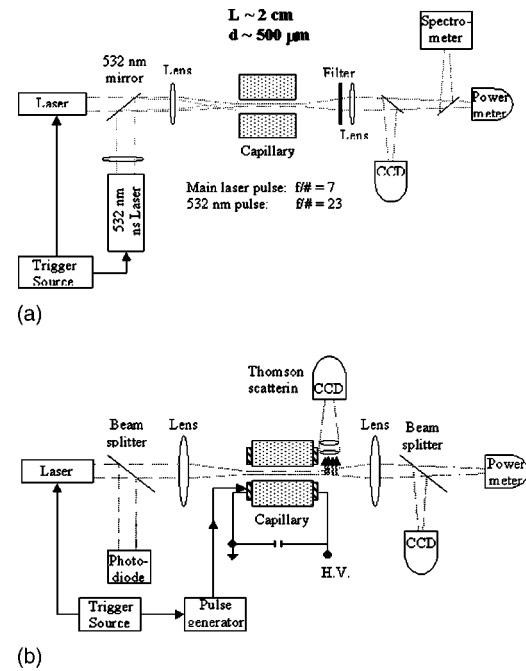


FIG. 2. (a) Experimental diagnostic setup with laser preionized capillary experiment. (b) Experimental setup for diagnosing optical guiding.

dynamically created.³² For intense laser guiding, the goal is then to send a guided pulse through the channel as it evolves through a density profile which is well mode-matched to the guided pulse.

The delay between the ablation pulse and the probe pulse was adjustable with subnanosecond jitter by triggering each laser’s Pockels cell with a low-jitter electronic delay generator. This delay could be arbitrarily adjusted, but was typically from 0 to a few tens of ns.

The focusing geometry and alignment of the ablating laser pulse with the capillary is critical to the uniformity of the plasma channel. Assuming an ablated plasma density proportional to the local laser fluence on the capillary surface, an ablation beam with large $f/\#$ is desirable for axial plasma uniformity. However, an upper limit on the $f/\#$ is determined by the maximum ablation pulse energy and the minimum ablation fluence required to produce a plasma. In addition, a large $f/\#$ requires more precise alignment of the ablation pulse with the capillary axis to avoid azimuthal asymmetry of laser fluence on the wall. The ablation pulse in our experiment was focused with $f/\# \sim 23$, yielding fluences on the capillary wall $\sim 10^{12}$ W/cm². The focus of the ablation pulse was placed a few mm in front of the capillary entrance, such that its diverging beam nearly filled the capillary entrance.

The setup for diagnosing optical guiding in both capillary discharge and laser-ablation experiments is illustrated in Fig. 2(b). The capillary was situated in a large vacuum chamber, which was evacuated using a turbomolecular pump. In all our experiments, the vacuum base pressure was 10^{-4} Torr or lower.

Our experiments utilized the T-cubed system, a high power Nd:glass laser system at the U.S. Naval Research Laboratory, to inject 400 fs, 1–2 TW laser pulses ($\lambda = 1054$

nm) into the capillary plasmas. The laser beam was focused by a 30 cm focal length BK7 lens at one end of the capillary and had an estimated focal spot size on the order of $20\ \mu\text{m}$. The effect of the plasma on the propagation of the laser beam was determined from measurements of the mode structure at the exit of the capillary by imaging the transmitted $1\ \mu\text{m}$ radiation onto a charge coupled device (CCD) camera. It is particularly important that measurements of the spatial mode quality of the transmitted laser pulse be made in order to determine how the parameters of the capillary plasma can be adjusted so that single mode propagation is possible. A measurement of the amount of energy passing through the capillary could be obtained by using a pyroelectric energy detector. Collection optics with $f/\# \sim 1$ were used to relay the transmitted light to the detector.

A direct consequence of optical guiding is an increase in the energy transmitted over a given length along the optical axis. A series of measurements of the output energy of the laser pulse after transmission through the capillary was made. Measurements of how output transmission varies with respect to input energy can provide information about losses due to inverse bremsstrahlung, scattering, refraction, and imperfections in the plasma gradients. It was found that the energy transmission efficiency $E_{\text{out}}/E_{\text{in}}$ of the capillary plasma for an optically guided laser pulse varied significantly with respect to laser injection timing, discharge duration, and energy, as previously observed.²⁴

III. STIMULATED RAMAN SCATTERING MEASUREMENTS

Previous work to examine the propagation of high intensity laser pulses has typically examined the output mode structure of the channeled laser beam and the amount of transmitted energy. While these parameters are clearly important, they do not provide sufficient information about the behavior of the high intensity laser radiation in the interior of the plasma channel. Simulations of the propagation of laser light in the plasma channel have not been confirmed experimentally since it is difficult to obtain data during propagation of the laser pulse through the channel on this time scale. Probing and imaging of the interaction region is difficult in plasma channels, and especially in capillary discharges, since access to the interior is limited. In particular, for applications of these channels it is important that the capillary is designed so that the interaction provides the most uniform region of high intensity radiation possible. It is also important to avoid catastrophic focusing and defocusing in the interior of the channel since the propagation of the laser may be significantly affected by ionization-induced refraction.

We have developed a temporally resolved stimulated Raman backscattering diagnostic in order to make quantitative measurements of both the instantaneous electron density and the instantaneous intensity of the laser pulse as it propagates through the plasma channel, and consequently to determine the optimal conditions for guiding.

Stimulated Raman scattering (SRS)³³ is a parametric instability in which an intense laser pulse scatters off a plasma oscillation driven by the same pulse. This plasma wave

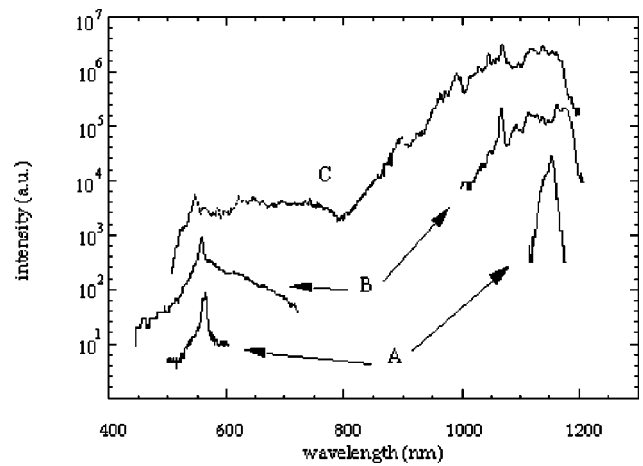


FIG. 3. Examples of stimulated Raman backscattered spectra at different intensities in the strongly coupled regime, for interactions without a plasma channel.

couples to the laser photon to produce a frequency downshifted backscattered photon, thus providing the positive feedback for the instability to grow.

In our experiments, we were interested in the channeling of extremely high intensity radiation. In order to determine the high intensity behavior of the SRS instability the backscattered light was measured by imaging the $\sim 4\%$ reflection from a bare glass beamsplitter onto the entrance slit of a spectrometer (0.25 m Jarrell–Ash Model 1233 with 150 lines/mm grating). The spectrometer was operational in the wavelength range 350–1200 nm using either a CCD array as the detector for time-integrated measurements, or a fast Cordin model 171 Proschon picosecond streak camera for time-resolved measurements. The experimental setup for backscattered SRS measurements is shown schematically in Fig. 6.

We initially observed time-integrated backscattered SRS spectra from interactions with helium gas jet plasmas of a known density.³⁴ This allowed an exploration of the intensity dependent characteristics of SRS. At relatively low intensity (up to $10^{16}\ \text{W}/\text{cm}^2$), the light directly backscattered by SRS shows a single narrow peak which is frequency-downshifted by the electron plasma frequency to $\sim 1140\ \text{nm}$ (spectrum A of Fig. 3). Here one can use the backscattered SRS shift ω_{pe} to measure n_e , where $\omega_{\text{SRS}} = \omega_0 - \omega_{\text{pe}}$ and ω_{pe} is the electron plasma frequency. The amount of this shift allowed a precise measurement of the plasma electron density during the interaction.

The spectra in Fig. 3 illustrate the intensity dependence of backscattered SRS. At intensities above $10^{17}\ \text{W}/\text{cm}^2$ a narrow peak at the second harmonic of the Raman scattered light ($\sim 570\ \text{nm}$) appears in the directly backscattered direction (spectrum A of Fig. 3), and is likely due to the interaction of the Raman backscattered light with large laser produced density gradients in the focal region of the laser.³⁵ As the laser intensity was increased to $1 \times 10^{18}\ \text{W}/\text{cm}^2$ (spectrum B of Fig. 3), the backscattered Raman peak is blue-shifted and becomes significantly broader. The backscattered second harmonic signal also broadens significantly. As the laser intensity increases to $2 \times 10^{18}\ \text{W}/\text{cm}^2$, the SRS spec-

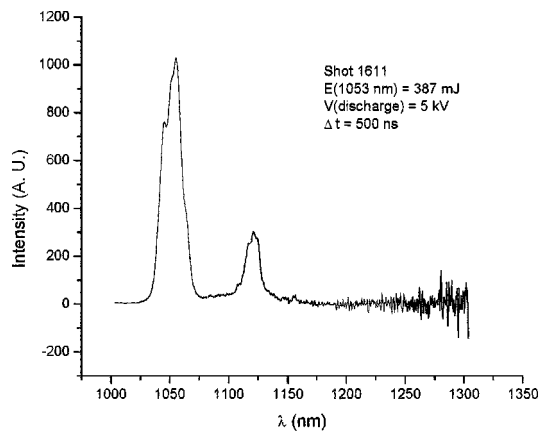


FIG. 4. A typical backscattered spectrum from capillary discharge experiment. Central frequency indicates that the average interaction density is $1.5 \times 10^{18} \text{ cm}^{-3}$.

trum and the second harmonic of the SRS spectrum become even broader so that the spectra merge and continuum-like emission is observed throughout the entire region (spectrum C of Fig. 3). Note that the spectra in Fig. 3 have been scaled to include the efficiencies of the spectrometer grating and the CCD detector. The duration of this backscattered emission was measured using a streak camera and it was found to be less than the temporal resolution of the instrument used (10 ps) and may be assumed to be concurrent with the duration of the passage of the laser pulse through the plasma. In this case the distance was less than 1 mm (on the order of the Rayleigh range). Total absorption and scattering of light by all processes at $I = 2 \times 10^{18} \text{ W/cm}^2$ and $n_e = 6 \times 10^{18} \text{ cm}^{-3}$ was measured to be not more than 15%. The amount of radiation scattered in the backscattered direction at intensities of $2 \times 10^{18} \text{ W/cm}^2$ was measured to be about 10%.

The source of the extreme broadening in the backscattered spectra is the high intensity limit of the SRS instability. For very high intensities a much wider spectrum of unstable plasma modes can couple to the scattered light (the strongly coupled regime). For high intensity short pulse laser physics, parametric instabilities such as SRS are only important when the growth time is much less than the length of the laser pulse. The SRS growth rate

$$\gamma = \frac{\omega_{pe}^2}{2\sqrt{2}\omega_0} \frac{\nu_{osc}}{c},$$

which is proportional to $\nu_{osc} \sim (I\lambda^2)^{1/2}$, yields an e-folding time of $\sim 5 \text{ fs}$ at $n_e = 1 \times 10^{19} \text{ cm}^{-3}$. This implies that for high intensity laser pulses of 0.5 ps duration this instability should be important and may reach saturation. Instability and saturation thresholds depend also on the density scale length and the damping rate of the plasma waves. The growth of the Raman scattered light beyond the linear regime has recently been examined in higher density plasmas where the reflectivity was found to saturate at about 10%.³⁶

For measurements of laser propagation in a plasma channel, time-integrated spectroscopy provides a simple prelude to time-resolved measurements. In Fig. 4 a typical time-integrated backscattered SRS measurement is shown resulting from the propagation of the high intensity laser pulse

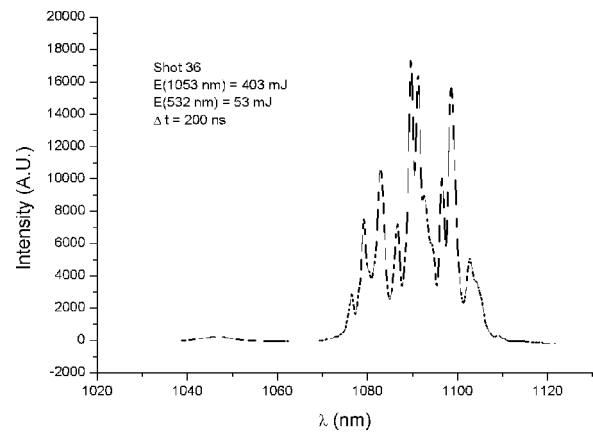


FIG. 5. A typical backscattered spectrum from a plasma channel preformed by a second laser pulse is shown. The frequency of the spectrum centroid indicates that the average interaction density is $1.4 \times 10^{18} \text{ cm}^{-3}$.

through a 2 cm length polyethylene capillary with a plasma channel formed by electrical discharge. For discharge-formed plasmas, longer delay times seemed to produce the highest density plasmas in the channel. Figure 5 shows a typical backscattered spectrum from a laser-preformed plasma channel. In the case where a second laser was used to preform the density profile, short delay times were found to produce the largest Raman shifts (and largest n_e). In addition, higher ablation pulse energies produced larger Raman shifts. For all our laser-ablated channel experiments, Raman shifts indicated a central plasma electron density of $n_e \leq 2 \times 10^{18} \text{ cm}^{-3}$. Previous measurements of capillary discharge plasmas suitable for optical guiding yielded densities at capillary ends, $n_e \sim 1 \times 10^{19} \text{ cm}^{-3}$.²⁴

IV. TEMPORALLY RESOLVED SRS DIAGNOSTIC

Subsequently, we measured the interaction of the intense laser pulse as it propagated through a plasma channel by temporally resolving the stimulated Raman backscattered signal. Since stimulated Raman backscattering at high intensity is an absolute instability in the laboratory frame, a temporally resolved measurement of the backscattered spectrum can provide information on the instantaneous plasma density inside the channel as well as the instantaneous laser intensity (i.e., the uniformity of propagation).

Figure 6 shows a schematic of the time-resolved backscattered SRS diagnostic setup. As the high intensity pulse

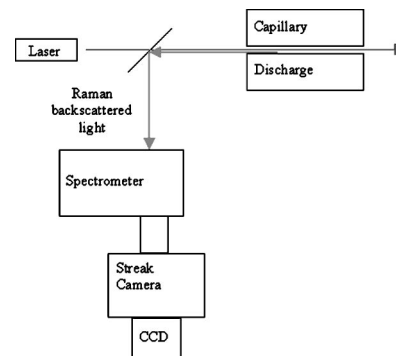


FIG. 6. Setup for temporally resolved Raman backscattering measurements.

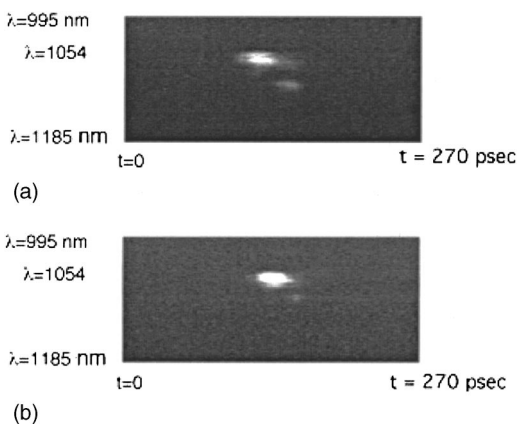


FIG. 7. Two temporally resolved backward scattered Raman spectra generated in capillary discharge plasmas are shown. In each, a reflection at the fundamental laser wavelength, 1054 nm, can be seen from the front surface of the capillary. A Raman Stokes satellite can be seen approximately 27 ps after this. The time delay of the Stokes satellite from the front surface reflection in both spectra corresponds to propagation of the probe beam approximately 4 mm into the capillary. In (a) the delay between discharge initiation and the probe pulse is 300 ns, with a Raman frequency shift corresponding to a plasma density $1.5 \times 10^{18} \text{ cm}^{-3}$. In (b) the delay between discharge initiation and the probe pulse is 50 ns, with a Raman frequency shift corresponding to a plasma density $1.0 \times 10^{18} \text{ cm}^{-3}$.

propagates through the capillary, light is Raman backscattered with a frequency shift corresponding to that of the local plasma density. The scattering region corresponds to the region instantaneously occupied by the laser pulse ($\sim 120 \mu\text{m}$ in length for our 400 fs pulse length). Consequently, the scattered Raman light pulse provides fine axial resolution in the record of local plasma density. The transit time of the laser pulse through the capillary is on the order of 65 ps for a 2-cm-long capillary. Backscattered light from a probe laser pulse makes a round trip from the entrance of the capillary to the scattering point, then back to the capillary entrance before continuing to the streak camera. Therefore, any backscattered signal at the streak camera would be stretched to 130 ps, twice the capillary transit time. The 2 ps peak time resolution of our streak camera was not attainable in our experiments due to jitter inherent in the triggering system. For data presented here, the effective time resolution was approximately 15 ps.

The amplitude of the backscattered signal can also give approximate information about the laser intensity. However, as discussed in Sec. III, in the strongly coupled regime it is also possible to use measurements of the bandwidth of the signal to determine laser intensity. Since the amplitude of the signal may be variable because of the requirement that the backscattered SRS is guided back out of the channel, the correlation of the amplitude of the backscattered Raman signal with the bandwidth can also indirectly provide a measurement of the evolution of the plasma channel after passage of the high intensity laser beam.

In order for this technique to be useful, the temporal resolution of the streak camera used also needs to be much greater than the time it takes for the laser pulse to pass through the plasma channel. Two temporally resolved backscattered spectra generated by a high intensity laser pulse propagating in a capillary discharge plasma are shown in Fig.

7. The light seen at the fundamental laser wavelength was a specular reflection of the outer wings of the beam from the front surface around the capillary entrance. This light therefore provided a fiducial mark, indicating the time of entry of the probe pulse into the capillary. Energy transmission and laser beam exit mode were not measured for these shots, so it is unknown whether they produced optical guiding.

The Stokes line of the SRS signal appears approximately 27 ps after front surface reflection with a 42 nm shift, indicating an electron plasma density of $n_e \sim 1.5 \times 10^{18} \text{ cm}^{-3}$. The time delay indicates that the laser pulse reached maximum intensity approximately 4 mm inside the capillary. Therefore, the region of high intensity was not axially uniform for this capillary design. No subsequent scattering peaks are observed. The beam appears to have been defocused after the scattering point, resulting in a sufficiently larger beam size and correspondingly lower intensity so that subsequent SRS backscattering was not generated.

The temporal width of the spectral peaks in Fig. 7 represent the camera resolution limit, likely determined by the resolution of the phosphor in the image intensifier. The apparent temporal width of the spectral peak of the laser fundamental is larger than that for the SRS peak, due to increased bloom of the phosphor at higher signal intensity.

The axial nonuniformity of the laser propagation may be due to several effects. A mismatch in transverse size of the laser beam with the plasma channel can result in betatron-like oscillations of the guided pulse. Careful design of the plasma channel density profile, as well as precise axial and transverse alignment of the focused laser pulse with the plasma channel entrance are therefore critical for uniform optical guiding. Also, axial and azimuthal nonuniformities in the capillary plasma density can cause localized pinching or asymmetric refraction of the guided pulse, again resulting in nonuniform pulse intensities.

A strong candidate cause for axially nonuniform intensity is ionization-induced refraction at high laser intensities. Ionization-induced refraction occurs when the leading edge of the pulse is sufficiently intense to field ionize the medium. This results in a plasma density maximum on the axis of laser propagation. Such a density profile acts as a defocusing lens for the trailing part of the laser beam. Note that in our experiments the focused intensity of the 1 TW laser pulse at the input aperture of the capillary is estimated to be about 10^{18} W/cm^2 , orders of magnitude larger than that required to photoionize H, C, and C^{1+} , which are typical major components of the capillary discharge plasma. Monitoring of forward-scattered guided pulse spectra for ionization-induced blue shift should provide valuable information in determining the role of ionization-induced refraction. Ionization-induced refraction is clearly an important issue for high intensity optical guiding in plasma channels.

Further work to determine the cause of axially nonuniform laser intensity, and to improve the characteristics of plasma channels for high intensity optical guiding is presently underway.

V. DISCUSSION

These measurements show that while capillary discharge-generated plasma channels can optically guide TW laser pulses over many Rayleigh lengths, pulse intensity may not be axially uniform. The data suggest that axial and azimuthal plasma density uniformity, as well as matching of the guided pulse beam size with the plasma channel width are important. Further, the data corroborate previous findings⁸⁻¹⁰ that ionization-induced refraction may play a critical role in the interaction between high intensity laser pulses and capillary discharge plasmas and may limit the intensity of channeled laser pulses unless careful consideration is given to the design of the experiment. An optimal plasma for high intensity optical guiding should therefore be fully ionized and, ideally, completely stripped.

In conclusion, the experiments described here have shown the usefulness of diagnosing high intensity laser propagation through plasma channels using time-resolved Raman backscattering. These proof-of-principle results indicate that the laser intensity in the channel was nonuniform in our experiments. This diagnostic technique should be applicable to a broad array of plasma channeling experiments such as capillary discharges, laser-ablated capillary plasma channels, glass capillary waveguides, and perhaps in fast igniter experiments where channeling is required in very high density plasmas.⁴ Further use of this diagnostic should enable accurate determination of the laser intensity throughout the plasma channel. Many applications of high intensity optically guided light require propagation with uniform intensity. This diagnostic will therefore be critical for determining requirements for a plasma waveguide, as well as evaluating plasma channel production techniques for optical guiding. Indeed, this diagnostic provides a powerful tool for successful application of plasma channels for high intensity laser guiding.

ACKNOWLEDGMENTS

The authors would like to thank R. F. Hubbard, B. R. Kusse, P. Sprangle, and A. Zigler for useful discussions. This work was supported by the U. S. Office of Naval Research, the U. S. Department of Energy, and the United Kingdom Engineering and Physical Sciences Research Council.

¹M. Perry and G. Mourou, *Science* **264**, 917 (1994).

²T. Tajima and J. M. Dawson, *Phys. Rev. Lett.* **43**, 267 (1979); P. Sprangle, E. Esarey, A. Ting, and G. Joyce, *Appl. Phys. Lett.* **53**, 2146 (1988).

³P. Amendt, D. C. Eder, and S. C. Wilks, *Phys. Rev. Lett.* **66**, 2589 (1991); N. H. Burnett and G. D. Enright, *IEEE J. Quantum Electron.* **QE-26**, 1797 (1990); B. E. Lemoff, G. Y. Lin, C. L. Gordon III, C. P. Barty, and S. E. Harris, *Phys. Rev. Lett.* **74**, 1574 (1995); K. Krushelnick, W. Tighe, and S. Suckewer, *J. Opt. Soc. Am. B* **13**, 306 (1996).

⁴M. Tabak, J. Hammer, M. E. Glinsky, W. L. Kruer, S. C. Wilks, J. Woodworth, E. M. Campbell, M. D. Perry, and R. J. Mason, *Phys. Plasmas* **1**, 1626 (1994).

⁵E. Esarey, P. Sprangle, J. Krall, and A. Ting, *IEEE Trans. Plasma Sci.* **24**, 252 (1996).

⁶A. B. Borisov, A. V. Borovsky, O. B. Shiryayev, V. V. Korobkin, A. M. Prokhorov, J. C. Solem, T. S. Luk, K. Boyer, and C. K. Rhodes, *Phys. Rev. Lett.* **68**, 2309 (1992); P. Monot, T. Auguste, P. Gibbon, F. Jakober, G. Mainfray, A. Dulieu, M. Louis-Jacquet, G. Malka, and J. L. Miquel, *ibid.* **74**, 2953 (1995).

⁷G. Z. Sun, E. Ott, Y. C. Lee, and P. Guzdar, *Phys. Fluids* **30**, 526 (1987).

⁸P. Monot, T. Auguste, L. A. Lompre, G. Mainfray, and C. Manus, *J. Opt. Soc. Am. B* **9**, 1579 (1992).

⁹W. Leemans, C. Clayton, W. Mori, K. Marsh, P. K. Kaw, A. Dyson, and C. Joshi, *Phys. Rev. A* **46**, 1091 (1992).

¹⁰S. Nikitin, Y. Li, T. Antonsen, and H. Milchberg, *Opt. Commun.* **157**, 139 (1998).

¹¹Y. R. Shen, *Principles of Nonlinear Optics* (Wiley, New York, 1984).

¹²E. Esarey, J. Krall, and P. Sprangle, *Phys. Rev. Lett.* **72**, 2887 (1994).

¹³G. Shvets and J. S. Wurtele, *Phys. Rev. Lett.* **73**, 3540 (1994); P. Sprangle, J. Krall, and E. Esarey, *ibid.* **73**, 3544 (1994).

¹⁴K. C. Tzeng, W. Mori, and C. Decker, *Phys. Rev. Lett.* **76**, 3332 (1996).

¹⁵R. F. Hubbard, D. Kaganovich, B. Hafizi, C. I. Moore, P. Sprangle, A. Ting, and A. Zigler, *Phys. Rev. E* **63**, 036502 (2001).

¹⁶A. Goltsov, D. Korobkin, A. Morozov, and S. Suckewer, *Plasma Phys. Controlled Fusion* **41**, 595 (1999).

¹⁷J. J. Rocca, V. Shlyaptsev, F. G. Tomasell, O. D. Cortazar, D. Hartshorn, and J. L. A. Chilla, *Phys. Rev. Lett.* **73**, 2192 (1994).

¹⁸H. M. Milchberg, C. G. Durfee III, and T. J. McIlrath, *Phys. Rev. Lett.* **75**, 2494 (1995).

¹⁹C. G. Durfee III and H. Milchberg, *Phys. Rev. Lett.* **71**, 2409 (1993).

²⁰P. Volfbeyn, E. Esarey, and W. Leemans, *Phys. Plasmas* **6**, 2269 (1999).

²¹W. W. Gaul, S. P. Le Blanc, A. R. Lundquist, R. Zgadzaj, H. Langhoff, and M. C. Downer, *Appl. Phys. Lett.* **77**, 4112 (2000).

²²K. Krushelnick, A. Ting, C. I. Moore, H. R. Burris, E. Esarey, P. Sprangle, and M. Baine, *Phys. Rev. Lett.* **78**, 4047 (1997).

²³S. Jackel, R. Burris, J. Grun, A. Ting, C. Manka, K. Evans, and J. Kosakowski, *Opt. Lett.* **20**, 1086 (1995).

²⁴Y. Ehrlich, C. Cohen, A. Zigler, J. Krall, P. Sprangle, and E. Esarey, *Phys. Rev. Lett.* **77**, 4186 (1996).

²⁵D. Kaganovich, A. Ting, C. I. Moore, A. Zigler, H. R. Burris, Y. Ehrlich, R. Hubbard, and P. Sprangle, *Phys. Rev. E* **59**, R4769 (1999).

²⁶J. J. Rocca, O. D. Cortazar, B. Szapiro, K. Floyd, and F. G. Tomasell, *Phys. Rev. E* **47**, 1299 (1993).

²⁷T. Clark and H. Milchberg, *Phys. Rev. Lett.* **78**, 2373 (1997).

²⁸E. Gaul, S. Le Blanc, A. Rundquist, R. Zgadzaj, H. Langhoff, and M. Downer, *Appl. Phys. Lett.* **77**, 4112 (2000).

²⁹D. Kaganovich, P. Sasorov, Y. Ehrlich, C. Cohen, and A. Zigler, *Appl. Phys. Lett.* **71**, 2925 (1997).

³⁰D. Kaganovich *et al.*, *Appl. Phys. Lett.* **75**, 772 (1999).

³¹A. Ting, K. Krushelnick, C. I. Moore, H. R. Burris, E. Esarey, J. Krall, and P. Sprangle, *Phys. Rev. Lett.* **77**, 5377 (1996).

³²T. G. Jones, C. I. Moore, A. Ting, P. Sprangle, D. Kaganovich, and K. Krushelnick, *Proceedings of the 2001 Particle Accelerator Conference, Chicago 2001*, Vol. 5, p. 3993.

³³W. L. Kruer, *The Physics of Laser Plasma Interactions* (Addison-Wesley, New York, 1988).

³⁴A. Ting, K. Krushelnick, H. R. Burris, A. Fisher, C. Manka, and C. I. Moore, *Opt. Lett.* **21**, 1096 (1996).

³⁵K. Krushelnick, A. Ting, H. R. Burris, A. Fisher, C. Manka, and E. Esarey, *Phys. Rev. Lett.* **75**, 3681 (1995).

³⁶C. Rousseaux, G. Malka, J. L. Miquel, F. Amiranoff, S. D. Baton, and P. Mounaix, *Phys. Rev. Lett.* **74**, 4655 (1995).